Cerebral Cortex, April 2020;30: 2691–2707

doi: 10.1093/cercor/bhz269
Advance Access Publication Date: 11 December 2019
Original Article

ORIGINAL ARTICLE

Adolescent Decision-Making Under Risk: Neural Correlates and Sex Differences

Ozlem Korucuoglu[1,*], Michael P. Harms[1], James T. Kennedy[1], Semyon Golosheykin[1], Serguei V. Astafiev[1], Deanna M. Barch[1,2] and Andrey P. Anokhin[1]

[1]Department of Psychiatry, Washington University School of Medicine, St. Louis, MO 63110, USA, [2]Department of Psychological & Brain Sciences, Washington University, 1 Brookings Drive, St. Louis, MO, 63130, USA

*Address correspondence to Ozlem Korucuoglu, Department of Psychiatry, Washington University School of Medicine, 660 S. Euclid, Campus Box 8134, St. Louis, MO 63110, USA. Email: korucuogluo@wustl.edu

Abstract

An increased propensity for risk taking is a hallmark of adolescent behavior with significant health and social consequences. Here, we elucidated cortical and subcortical regions associated with risky and risk-averse decisions and outcome evaluation using the Balloon Analog Risk Task in a large sample of adolescents ($n = 256$, 56% female, age 14 ± 0.6), including the level of risk as a parametric modulator. We also identified sex differences in neural activity. Risky decisions engaged regions that are parts of the salience, dorsal attention, and frontoparietal networks, but only the insula was sensitive to increasing risks in parametric analyses. During risk-averse decisions, the same networks covaried with parametric levels of risk. The dorsal striatum was engaged by both risky and risk-averse decisions, but was not sensitive to escalating risk. Negative-outcome processing showed greater activations than positive-outcome processing. Insula, lateral orbitofrontal cortex, middle, rostral, and superior frontal areas, rostral and caudal anterior cingulate cortex were activated only by negative outcomes, with a subset of regions associated with negative outcomes showing greater activation in females. Taken together, these results suggest that safe decisions are predicted by more accurate neural representation of increasing risk levels, whereas reward-related processes play a relatively minor role.

Key words: BART, effect size, fMRI, insula, parametric design

Introduction

Adolescence is a period of transition from childhood to adulthood involving major physical, social, and psychological changes. A hallmark of adolescent behavior is an increased propensity for risk taking characterized by a preponderance of seeking and preferring rewards over avoiding punishments (Eaton et al. 2012). This imbalance between appetitive and aversive motivations and behaviors may result in a bias in decision-making processes (Cauffman et al. 2010). A moderate level of risk taking may be beneficial during adolescent development because it facilitates independent decision-making and learning based on trial and error, allowing adolescents to explore new physical and social environments and seek opportunities. However, taking risks that are associated with adverse consequences (i.e., seatbelt nonuse, condom nonuse, drug and alcohol use, smoking) frequently in adolescence can contribute to many problems later in life. Indeed, previous work suggests that higher levels of risk taking in adolescence (acts of aggression/larger number of sexual partners associated with greater domestic violence perpetration/victimization) are associated with poor health-related outcomes (O'Donnell et al. 2009). A substantial body of evidence summarized in multiple reviews (Boyer 2006; Steinberg 2004) indicates an increase of risk-taking behavior in both real-life and experimental settings during adolescence, although the evidence that risk-taking peaks in adolescence is less consistent. Additional research using large,

population-representative longitudinal samples is needed for a more definitive answer to the question of whether adolescents are more likely to take risks and suffer adverse health-related consequences as a result of risk taking than young adults. Furthermore, studies suggest that social context may play a greater role in adolescent risk-taking than age differences in risk perception or appraisal (Steinberg 2004). The ability to pursue risk appropriately at this age is central for the emergence of healthy behaviors in adulthood. Education and intervention programs, aimed at moderating risk-taking behavior in adolescence, will benefit from a better understanding of the neural and cognitive mechanisms underlying risky and risk-averse decision-making.

One potential mechanism of maladaptive risk taking may involve poor representation of the degree of risk, particularly in situations where the degree of risk (i.e., the probability and magnitude of potential harmful consequences) gradually increases together with the magnitude of a potential good outcome when the exact odds of negative outcomes are not explicit. This definition of risk is the colloquial notion of "risk" used in this paper (in contrast to "risk" solely a change in the probability of a different outcome, as defined in some previous neuroeconomic research [Huettel et al. 2006; Levy et al., 2010]). Probability and magnitude information must be integrated to choose options with the highest expected values (see Glimcher 2008 for a review). However, it has been shown that individuals do not combine probability information linearly with magnitude information (Berns et al. 2008). Krain et al. (2006) state that risky decisions with low probabilities of gaining a larger reward are more affectively laden and distinct from situations of decision-making under uncertainty, in which probabilities are unknown but outcomes have equal value. Poor representations of risk might be insufficient to terminate a high-risk behavior, or alternatively, an increased sensitivity for potential rewards might outweigh the "brake mechanism," rendering the ongoing behavior maladaptive. In this type of situation, two scenarios are possible. In the case of an adaptive (risk-aversive, or safe) decision, the trade-off between magnitude of a potential reward and probability of a negative outcome will eventually trigger the inhibitory control process and result in the avoidance or termination of the behavior. In the case of maladaptive (risky) decision, a failure to adequately represent the increasing degree of risk or an increased sensitivity for the high payoffs or both will result in persistent risky choices. However, brain mechanisms that are involved in processing variations in the magnitude and probability of risk are not yet understood. Until now, only a few studies looked at brain activation as a function of degree of risk in adults. In these studies, risky choices with increasing degree of risk or consecutive risky choices were associated with anterior cingulate cortex (ACC) activation, whereas safe (risk-averse) choices engaged both ACC and insula (Fukunaga et al. 2012; Schonberg et al. 2012). One study in a small sample of youth (23 youths with familial risk for substance use and 27 controls, between 10 and 14 year olds) failed to identify any regions involved in risky or risk-averse decisions that are sensitive to the degree of risk (Hulvershorn et al. 2015). It is important to note that the scenarios of "maladaptive versus adaptive decisions" described above represent extreme manifestations of risky and risk-averse behaviors, whereas we assume that individual differences in the neural representation of the degree of risk/reward and its impact on decision-making show a continuous (dimensional) distribution in the general population.

Maturation-related changes of the adolescent brain provide a biological basis for the changes in risk-taking behaviors. Current neuroscience perspectives on adolescent risk taking postulate that the developmental imbalance between a slowly maturing regulatory processes (in particular, inhibition), involving the inferior frontal and anterior cingulate cortices, and faster maturing reward-motivational processes including the ventral striatum and amygdalae, underlies the suboptimal decision-making in adolescence (Jentsch and Taylor 1999; Casey et al. 2008; Somerville et al. 2010). Compared to adults, adolescents were reported to exhibit increased activity of the striatal and limbic system to large rewards suggesting greater sensitivity of these regions to larger rewards, with a peak reward response occurring around the age of 14–15 (Doremus-Fitzwater et al. 2010; Galvan 2010). However, a second line of research has shown that adolescents are not more risk seeking than adults when the precise odds of each possible outcome are known, but show greater tolerance for options with unknown probabilities (Tymula et al. 2012). While one study showed a linear decrease in ambiguity tolerance with age between 10–25 years (Blankenstein et al. 2016), another study identified a quadratic trend peaking at 15–16 years (van den Bos and Hertwig 2017). Accumulating evidence suggests that adolescents' brain responses to risk may be better captured under conditions when the probabilities of good and bad outcomes are not explicit, which is typical for most real-life situations with potentially adverse consequences (drug use, reckless driving, unprotected sex, etc.). Moreover, risky behaviors with known and unknown probabilities seem to be driven by different neural mechanisms. Although adolescent tendency to engage in risk taking under ambiguity (unknown probabilities) was associated with reduced dorsomedial prefrontal cortex (DMPFC) and insula activation, risky gambles with known probabilities were associated with ventral striatal activation and may be triggered by the reward valuation (Blankenstein et al. 2018). Exploring personal limits is another important feature of adolescent behavior that needs to be examined experimentally using a design that can delineate the switching point from a risky to a safe choice as a function of increasing possible risks and rewards. This type of decision-making also invokes a sense of escalating tension and exhilaration, emulating risk taking in naturalistic environments (Schonberg et al. 2011) and may explain the power of such paradigms in predicting adolescent real-world risk-taking behaviors (Lejuez et al. 2002; Hunt et al. 2005). Lastly, recent neuroscience models attribute sex differences in risk preferences to divergent and permanent reorganization of brain circuits during adolescence in boys and girls, partially driven by differential effects of sex hormones in the brain (Vigil et al. 2016).

Previous neuroimaging studies of risky and risk-averse decision-making reported variable results with respect to patterns of regional brain activation and sex differences, which may be a result of the modest sample sizes used in most studies. Decision-making in general has been associated with activity in orbitofrontal cortex (OFC), rostral portions of ACC, dorsolateral prefrontal cortex (DLPFC), parietal cortex, thalamus, and caudate (see Krain et al. 2006 for a meta-analysis and Ernst and Paulus 2005 for a review). However, findings are variable and include reports of both hyperactivations and hypoactivations in the insula (Duijvenvoorde et al. 2015; Kim-Spoon et al. 2017) and ventral striatum (Bjork et al. 2010; Geier et al. 2010). Interestingly, the insula has also been shown to be activated to a greater extent in females compared to

males (Lee et al. 2009). Well-powered fMRI studies of risky decision-making in adolescents are scarce. Although there are ongoing Big Data studies on adolescent brain development—such as adolescent brain cognitive development (ABCD) study (Casey et al. 2018), no risk-taking tasks are included in their scanning protocols. Furthermore, most previous studies investigated risk as a function of probability of outcomes rather than in the context of sequential risky choices with increasingly high rewards and losses at stake (Eshel et al. 2007; Van Leijenhorst et al. 2010). Furthermore, given that sex hormones influence development of adolescent neural circuitry and affect emotions (Vigil et al. 2016), experimental research should aim to explain whether and how substantial sex differences in risk-taking behavior that emerge during adolescence are reflected in divergent patterns of brain activity. Finally, there has been little discussion in the neuroimaging literature on risk taking regarding whether risk-taking paradigms modified for the use in the scanner, in which the increased risk is paired with an increased reward in a single response, capture the same inhibitory control processes and risk preferences as out-of-scanner behavioral risk-taking paradigms, in which the gain is fixed, such as the widely used Balloon Analog Risk Task (BART) (Lejuez et al. 2002). Few previous studies examined convergent validity of the different task versions. Therefore, in the current study, subjects were tested with both versions of the task.

The current study attempts to address these open questions by using a large ($n = 256$), population-representative sample of adolescents, permitting the detection of even moderate effect sizes, controlling for potential confounders, and examination of the effects of demographic variables such as sex and its interaction with task conditions. Specific aims of the present study were (1) to characterize patterns of brain activation involved in decision-making processes in adolescents and identify brain regions that are involved in risky decision-making versus regions that are specifically sensitive to the increasing degree of risk, (2) to examine sex differences in risk-taking and risk-averse behaviors and the corresponding patterns of brain activation in adolescence, and (3) to provide evidence as to whether the same cognitive processes were being engaged while measuring decision-making processes in behavioral and neuroimaging modalities.

Risk taking in the scanner was measured with a modified version of BART (Rao et al. 2008), in which participants are given the chance to earn money by sequentially inflating a balloon without popping it. Compared to other decision-making tasks used in neuroimaging, this task investigates risk behaviors in a sequential manner, in which risky and risk-averse decisions are made in the context of a trade-off between probability and amount (magnitude), with the overall level of risk being strongly tied with the level of reward, similar to many real-life situations. We modeled the neural activity during selection of risky versus safe choices in two ways: as an overall effect (average neural activity modeled with the use of a categorical design) and as a function of increasing degree of risk (parametric modulator). Owing to the parametric relationship between the levels of risk in successive pumps of the balloon, risk/reward in this task can be modeled as a covariate, and we can identify brain regions that respond to parametric manipulations of reward and loss. Similar to real life situations, in a sequential decision-making task like BART, later (inflation) choices entail greater risk taking than early choices. Similarly, late "cash-out" decisions avoid greater losses and, therefore, represent an increasingly aversive response (Fukunaga et al. 2012). Thus, the parametric model assists in identifying brain regions that are not only involved in decision-making under risk, but also in regions related to increasing levels of risk-taking/reward-seeking (for the inflation choices), or risk-avoidance behavior (for the cash-out choices).

We systematically reviewed the fMRI literature that utilized BART to identify all the relevant regions that may play a primary or secondary role in risky decision-making (see Supplementary Table S4). Given the literature reviewed, we hypothesized that the anterior insular cortex (AIC) activation would track the increasing degree of risk, ACC would be involved in both in the choice of risky and safe decisions, vmPFC would be involved due to its role in integration of information, and the dlPFC and IFG due to their contributions to self-control and inhibition.

Materials and Methods

Participants

A sample of 260 participants, consisting of 126 boys and 134 girls (mean_{Age}: 14.15 years, (standard deviation) SD_{Age}: 0.6) were included in the current analysis. The original sample included 280 adolescents between the ages of 12.7 and 15.5 years, recruited as part of a longitudinal twin study of genetics, neurocognitive development, and risk for psychopathology and substance abuse (see Supplementary Materials for exclusion criteria and demographic information). The BART was included in the scanning protocol at a later stage; therefore, for 270 subjects, the data from BART were available. Ten of the 270 subjects were excluded from the behavioral analysis and 14 subjects from the fMRI modeling for the following reasons: Seven fMRI naïve youth became cognizant of their claustrophobia at the day of the scanning session, two youth were not scanned because their twins were claustrophobic, and one youth's behavioral data were lost. Due to low performance, two youths did not have enough events for fMRI modeling and two youths were excluded due to problems with the scan data (Transformation of scans to standard space failed for one youth, and the BART of the other youth was aborted in the scanner.) The behavioral and fMRI analysis were completed with the remaining 260 and 256 participants, respectively. Study participants were identified through the Missouri Family Registry based on birth records.

The data presented here are part of their first baseline laboratory visit lasting 6–7 h. The Human Research Protection Office at the Washington University School of Medicine approved the study. A written informed consent was obtained from a parent or legal guardian of all the participants, and a written informed assent was obtained from the adolescent participants. Participants were compensated for participation in the study.

Procedure

Upon arrival in the lab, participants completed a behavioral testing session and an fMRI session, with the order depending on the scheduling of the scanner. Among 254 subjects who completed the out-of-scanner BART task, 123 of these completed the behavioral session first (14 of those on a different day) and 132 of these completed the scan session first (50 of those on a different day). During their behavioral session, participants completed out-of-scanner computer tasks including the BART (Lejuez et al. 2002; Hunt et al. 2005), a semistructured diagnostic interview, and self-report questionnaires. Before the actual scanning, participants were placed in a mock scanner for

accommodation to the scanner environment, where they performed practice versions of tasks administered during the scanning session, among which BART was the last (see Supplementary Materials for a description of practice session). Practicing the in-scanner BART in the mock scanner before the scanning session also mitigates the possibility of any influence of out-of-scanner version of BART.

Out-of-Scanner BART Description

In the original BART paradigm (Lejuez et al. 2002; Hunt et al. 2005), participants were given the chance to earn money by inflating a blue balloon presented in the center of a computer screen without popping it. With each pump, they could earn 1 cent, or they could stop inflating the balloon and cash-out the amount accumulated for the current balloon into a virtual bank at any time. However, the balloons could explode unpredictably at varying degrees of inflation, in which case the accumulated gain for the current balloon would be lost, but the amount that had previously been cashed-out into the bank was unaffected. The task included 30 balloons with a breakpoint of 64 pumps (corresponding to the task with blue balloon trials used in Hunt et al. 2005; adapted from Lejuez et al. 2002). Earlier research suggests that adding additional trials beyond 30 balloons results in little change in risk taking (Wallsten et al. 2005). Overall, girls and boys in our study had (on average) 29 and 35 adjusted pumps, greater than previous reports of 25.5 (for women) and 33.5 (for men) adjusted pumps in adults (Lejuez et al. 2002) and in line with previous reports of 35 adjusted pumps (on average) in adolescents (Lejuez et al. 2007). When the balloon was pumped beyond this point, a "pop" sound was generated with the presentation of an exploded balloon and all the money for that balloon was lost. The next trial started with the presentation of a new uninflated balloon. Subjects were informed that they would be given 30 balloons to inflate. Out-of-scanner BART took approximately 7 min to complete (range 5–10 min). Subjects received the total winnings from this task as an extra bonus, in addition to the compensation for study participation.

The outcome variables were the following: (a) *AdjustedPumps* refers to the average number of pumps made in the task for the cashed-out balloons and is typically considered as the main measure of risk taking in BART (Lejuez et al. 2002), (b) *TotalPumps* refer to the total number of pumps made in the task for both cashed-out and exploded balloons, (c) *N_Cashouts* refer to the number of cashed-out balloons, (d) *N_Explosions* refer to the number of exploded balloons, and (e) *AveragePumpsExplosions* refers to the average number of pumps made in the task for the exploded balloons. We also provided the following reaction time measures: (a) *RT_Cashouts*, (b) *RT_Pumps*, (c) *RT_PumpsCashouts*, and (d) *RT_PumpsExplosions*. This terminology was adapted to keep the outcome variables consistent across the in-scanner and out-of-scanner BART. Among 260 of our participants, 254 of them completed the behavioral BART.

In-Scanner BART Description

For the fMRI part of the present study, we used a scanner version of the BART developed by Rao and colleagues (Rao et al. 2008) (also see Supplementary Figure S1) for use in the scanner that differed from the original BART in the following respects: a maximum of 12 inflations were possible for each balloon. The probability of explosion and possible earnings across pumps increased monotonically (see Supplementary Table S2 for probability of explosions and possible earnings by number of inflations, Pearson r between P [explosion] and reward value = 0.99); all balloons (trials) had the same sequence of explosion probabilities; the total task duration was set to 10 min (acquired over a single run), during which subjects completed as many trials as possible (variable called *Balloons completed*); the task started with a fixation period of 30 s. A trial started with a balloon and a green rectangular cue, during which subjects had unlimited time to respond (a button press with index finger to pump the balloon or with the middle finger to cash-out triggers the onset of delay period). Following the response, the balloon remained on the screen for 0, 2, 4, or 6 s during which the balloon size did not change. The duration of the delay following the pump was randomly decided and each delay interval was given an exponentially decreasing weight (30, 12, 5, and 2, respectively). The participant's response could led to three possible outcomes: (1) if the subject cashed-out, the text "You Win" was presented for 1 s; (2) if the subject pumped the balloon and the balloon exploded, an exploded balloon was presented for 0.5 s, followed by the text "You Lose" for 1 s; and (3) if the balloon inflated successfully, the color of the rectangular cue switched to red for an equiprobable 1.5, 2, or 2.5 s. During the red cue period, subjects were instructed not to give any responses. After explosions or cash-outs, but before the next balloon appeared on the screen, a blank screen was presented for an equiprobable 2, 3, or 4 s (the interstimulus interval; ISI). The value of the current pump was displayed on the balloon and the total amount of winnings across task was displayed under the rectangular cue at all times when the balloon was visible. Another outcome variable specific to the scanner version of the BART was the *% Explosion Rate* referring to the ratio between the total number of exploded balloons and total number of balloons completed. Participants were paid their earnings at the end of the task. Subjects were informed that the task takes 10 min to complete.

fMRI Data Acquisition

Echo-planar imaging (EPI) of the whole brain was acquired with a 32-channel head coil on a 3 T Siemens MAGNETOM Prisma scanner in the WUSM Neuroimaging Labs, using Human Connectome Project (HCP) style acquisitions adapted for the ABCD study. The specific sequence implementations were the same as those used for the ABCD study (Casey et al. 2018). Structural scans included a sagittal-magnetization-prepared gradient-echo (MP-RAGE) T1-weighted image (repetition time [TR] = 2500 ms; echo time [TE] = 2.88 ms; flip angle = 8°; voxel size = 1.0 × 1.0 × 1.0 mm) and a sagittal T2-weighted image (TR = 3200 ms; TE = 565 ms; voxel size = 1.0 × 1.0 × 1.0 mm). Both the T1w and T2w scans utilized embedded volumetric navigators that detected and compensated for head movement in real time, with an allowance for reacquisition of the lines (TRs) in *k*-space that are heavily corrupted by motion (up to 24 TRs for the MP-RAGE and 18 TRs for the T2-SPACE scan). The combination of real-time motion correction and *k*-space reacquisition improves the quality of the structural scans and reduces the need for rescans, especially for age groups with a higher incidence of head movement (Tisdall et al. 2012). BOLD contrast for the task was measured with a gradient-echo EPI sequence (TR = 800 ms; TE = 30 ms; 60 contiguous 2.4-mm transversal slices; 2.4 × 2.4 mm in plane resolution, multiband factor 6, posterior-to-anterior phase encoding). Two brief spin-echo EPI scans with opposite phase-encoding

directions (anterior–posterior and posterior–anterior) were acquired before each EPI sequence scan for the purpose of correcting susceptibility distortion.

fMRI Data Processing

The HCP data analysis pipelines (https://github.com/Washington-University/HCPpipelines, v. 3.19.0) were used for the analysis of fMRI images (Glasser et al. 2013). The following pipelines were used: three structural preprocessing pipelines (*PreFreeSurfer*, *FreeSurfer*, and *PostFreeSurfer*) and two functional pipelines (*fMRIVolume* and *fMRISurface*). The main purpose of *PreFreeSurfer* pipeline is to generate an undistorted "native" structural volume space for each subject, align the T1w and T2w images, perform B1 (receive-coil bias field) correction, and register the subject's native structural volume space to MNI space. The *FreeSurfer* pipeline used FreeSurfer version 5.3.0-HCP. The main purpose of this pipeline is to segment the volume into predefined structures, reconstruct white and pial cortical surfaces, and compute FreeSurfer's standard folding-based surface registration. Finally, the *PostFreeSurfer* pipeline produces all of the NIFTI volume and GIFTI surface files necessary for viewing the data in Connectome Workbench, creates myelin maps, and applies the surface registration (including down sampling to a lower resolution, common mesh). Surface registration across subjects that used FreeSurfer's folding-based registration—"MSMSulc" registration (a more gentle folding-based alignment with less distortion; Robinson et al. 2018) was not used because the necessary "msm" binary was not publicly available at the time we started processing. Following the structural pipelines, all data underwent a careful quality control (see Supplementary Materials). The *fMRIVolume* preprocessing pipeline includes correction for gradient nonlinearities, volume realignment to compensate for subject motion, EPI distortion correction, bias field reduction, brain-boundary-based registration of EPI to structural T1-weighted scan, nonlinear (FNIRT) registration into MNI152 space, grand-mean intensity normalization and masking the data with the final brain mask. The *fMRISurface* pipeline transforms the time series from the volume into the CIFTI (Connectivity InFormatics Technology Initiative) grayordinate standard space (with cortical gray matter surface vertices and subcortical gray matter voxels, but excluding white matter and CSF). Surface-based registration for the cortical data improves the alignment of task-evoked data across subjects (Coalson et al. 2018). The HCP *TaskfMRIAnalysis* pipeline, which uses FMRIB's Expert Analysis Tool (FEAT) from FSL v6.00 (Jenkinson et al. 2012), was used to analyze cortical and subcortical grayordinate data for task modeling. The first eight frames were discarded from further analysis to allow for equilibrium of the longitudinal magnetization.

For task modeling, we used two distinct approaches: *categorical modeling* of BOLD responses to different event types (categorical design) and *parametric modeling* in which the probability of explosion was used as parametric modulator (parametric design). Figure S1 and Table S3 in the supplementary materials demonstrate the sequence of events and list of EVs in the task for cashed-out and exploded balloons.

The categorical model included three choice-related and four outcome-related regressors. Choice-related regressors included *ChooseInflate-Gain and ChooseInflate-Explosion* regressors preceding pumps—one for balloons that were subsequently cashed-out (gain) and one for balloons that were subsequently exploded (explosion)—and a *ChooseCashout* regressor. Outcome-related regressors included *OutcomeExplosion* and *OutcomeWin* regressors, plus *OutcomeInflate-Gain and OutcomeInflate-Explosion* regressors for successful pumps, for balloons that were subsequently cashed-out versus balloons that subsequently exploded, respectively.

Choice-related regressors were modeled with a duration (prior to convolution with the hemodynamic response function) equal to the interval from the onset of the green rectangular cue until the response. The *ChooseInflate-Gain* regressor preceding cash-outs included all pumps except the last balloon for which the subject pressed the cash-out button. Similarly, the *ChooseInflate-Explosion* regressor included all pumps before the explosion; this included the last balloon before explosion. *OutcomeInflate-Gain* and *OutcomeInflate-Explosion* regressors were modeled with a duration equal to the red rectangle cue presentation. The *OutcomeExplode* regressor included the duration of the presentation of exploded balloon plus the presentation of the"You Lose" feedback (i.e., 1.5 s total). The duration of the *OutcomeWin* regressor was always 1 s (the duration of the "You Win" feedback. *ChooseInflate-Explosion* and *OutcomeInflate-Explosion* events were included in the analysis as "conditions of no interest." Inclusion of pumps preceding explosions would have resulted in the inclusion of trials in which participants were forced to stop pumping because of explosion.

The categorical model included four contrasts as compared to the implicit baseline. These were: (1) ChooseInflate (preceding cash-outs, i.e., ChooseInflate-Gain regressor vs. baseline), (2) ChooseCashout, (3) OutcomeInflate (the presentation of inflated balloon, preceding cash-outs; i.e., OutcomeInflate-Gain regressor vs. baseline), and (4) OutcomeExplode. False discovery rate (FDR) corrected activation maps for the contrasts comparing events directly for the decision and outcome periods are provided in Supplementary Materials (see Figure S4).

In the parametric model, the probabilities of explosions [P (explode)] were included as a parametric modulator: within a regressor, each instance of an event was modeled together with its corresponding probability of explosion (i.e., 4.2% probability of explosion for pump number 3). The parametric model included all the same regressors and contrasts as the categorical model, except the *OutcomeWin* regressor included as nonparametric regressor, because the probability of explosion was no longer applicable at this point.

Group maps were created by using permutation statistics as implemented in PALM toolbox, version alpha101 (Permutation Analysis of Linear Models, http://fsl.fmrib.ox.ac.uk/fsl/fslwiki/PALM; Winkler et al. 2014). Multilevel exchangeability blocks (Winkler et al. 2015), which limit the permutations within block level (i.e., between two monozygotic –MZ- or two dizygotic –DZ- siblings), were used to handle the shared variance between twins in an appropriate manner. Vertex-wise statistics were corrected by PALM with FDR of $P < 0.05$, with 5000 permutations for each contrast. We did not correct for the multiplicity of contrasts. For anatomical labeling, the Human Connectome Project MultiModal Parcellation version 1.0 (HCP-MMP1.0) cortical parcellation Glasser et al. 2016) and the group-level Freesurfer subcortical segmentation encoded into the HCP standard CIFTI space were utilized.

Region of Interest Selection and Analysis

The purpose of selecting r**egion of interests (**ROIs) was twofold: To our knowledge, compared to previous studies of the BART, the current study has the largest sample size and hence the

high statistical power. Our first goal was to provide a list of the most prominent ROIs that can be targeted in future studies. Our second goal was to examine sex differences in the most prominent ROIs and to study the relationship between BOLD response amplitudes and behavioral performance for both the in-scanner and out-of-scanner BART. In this ROI selection process, we applied a stepwise procedure: first, we identified all regions that survived FDR-corrected thresholding and had a moderate-to-high effect size (for complete description of ROI selection protocol, see below); next, we selected a subset of these regions as an ROI if they were reported in previous decision-making/risk-taking meta-analysis [Krain et al. 2006, Tables 2 & 4; Silverman et al. 2015, Tables 2, 3 & 4] and/or in previous BART fMRI studies (for a complete list of these regions, see Supplementary Table S4).

The following protocol was used for the ROI selection: First, clusters were defined as groups of spatially contiguous vertices/voxels exceeding 80 mm^2/120 mm^3 (surface/volume for cortical and subcortical regions, respectively) from the whole-brain grayordinate-wise FDR-corrected group maps (see Figure S3). The FDR-corrected significant clusters were subdivided into ROIs by using the aforementioned parcellations, so that each ROI respected the parcellation boundaries (and thus was entirely inside one of the parcels). Second, ROIs for further analysis were selected by (a) requiring a Cohen's d value > 0.35 (small/medium) for cortical and > 0.2 (small) for subcortical regions for the categorical design and Cohen's d > 0.2 for the cortical and subcortical regions identified by the parametric design (according to Cohen's effect size classification, d = 0.2 is a "small" effect, and d = 0.35 is midway between the small and the "medium" effect of d = 0.5)[1] (see Figure 2); (b) requiring that significant activation was present in > 50% of the parcel/segment; (c) requiring that activation in that location had been reported in previously published fMRI studies of the BART (see Supplementary Materials and Supplementary Table S4 for details) and two meta-analyses results of risk taking/decision-making [Krain et al. 2006, Tables 2 & 4; Silverman et al. 2015, Tables 2, 3 & 4]; and (d) excluding any ROIs in the primary visual cortex as nontask-specific regions of activation consistently observed in most visual tasks.

Mean BOLD response magnitudes ("beta weights"; i.e., parameter estimates computed by the *TaskfMRIAnalysis* pipeline) were extracted from each segment for further analysis. We acknowledge that the method described above may have biased sex differences in the direction of type 2 error, given that regions with large sex differences may not survive our criteria of ROI selection. Therefore, we first conducted a whole brain analysis testing for sex differences; however, no regions survived the multiple comparison corrections of FDR at $P < 0.05$ for 91 252 vertices/voxels and number of contrasts. Next, we conducted an exploratory analysis on sex differences this time on the average beta weights per parcel/segment with the use of t-tests (Matlab function "*ttest2*"). These tests were FDR corrected for 360 MMP1.01 parcels and 19 Freesurfer segments ($P < 0.05$) with the use of a Matlab function ("*fdr_bd*") based on (Benjamini and Hochberg 1995) and (Benjamini and Yekutieli 2001). Independent samples t-tests examining sex differences on the selected ROIs (based on FDR-corrected maps, effects size and previous literature) are not corrected for multiple comparisons. The results of correlations between selected ROIs and BART performance can be found in the Supplementary Materials (see Tables S13 and S14).

Outlier Detection and Exclusion

All behavioral variables and selected ROIs were subjected to an outlier detection procedure implemented in R (https://www.R-project.org/). For the outlier detection procedure only, raw values were converted to Z-scores, and then values greater than three SDs from zero were recoded as missing values. This procedure was reiterated 10 times as outlier removal changes the shape of the distribution, allowing for the emergence of new outliers. With this exclusion procedure, 3.29% of the data was replaced with missing values from all selected cortical ROIs, 4.66% from all selected subcortical ROIs, 2.14% and 2.83% from all variables of the out-of-scanner and in-scanner BART, respectively (applied to variables listed in Table 2).

Group Comparison: Sex Differences

Outcome variables from in-scanner and out-of-scanner versions of the BART, average beta weights of the selected ROIs from the fMRI results were subjected to a group comparison (boys vs. girls) using independent sample t-tests.

Results

Performance Results

Task-Order Effect

We compared behavioral variables of the in-scanner and out-of-scanner BART task between participants who completed "behavioral session first" versus "scan session first" and also between participants who completed the behavioral and scan sessions "on the same day" versus "on separate days," with the use of independent samples t-tests. A significantly slower reaction time in the out-of-scanner task was observed among participants who completed in-scanner BART first, for the pumps preceding explosions (RT_PumpsExplosions, $P = 0.024$) and for all pumps (RT_pumps, $P = 0.045$). There was no significant effect of task order on any of the performance variables of the in-scanner BART, although there was a small nonsignificant trend toward greater number of average adjusted pumps in the in-scanner BART task among participants who completed out-of-scanner BART first, (5.48 vs. 5.27 pumps, $P = 0.052$, effect size = 0.24). We do not expect this difference to be due to performing out-of-scanner BART first for the following reasons: (1) before the fMRI session, subjects were extensively trained to be familiarized with the differences in the in-scanner BART task contrary to out-of-scanner BART task. Therefore, if

1 Due to the large sample in the current study and hence high statistical power to detect even small-size effects, significant activation encompassed widespread areas of the brain, warranting the use of further thresholding by effect size in order to focus the analysis on the most prominent regions. These thresholds were selected after the inspection of the activation maps in order to select spatially confined regions with the largest effect size. We used different effect size thresholds for cortical and subcortical regions and for the two designs (categorical and parametric) because of large differences in the overall activation magnitude and effect size (cortical greater than subcortical, categorical greater than parametric). Using the same threshold would preclude the identification of regions, for example, applying a threshold that is optimal for discrimination of subcortical regions to the cortical regions would result in clusters of activation spanning > 50% of a hemisphere. Conversely, applying thresholds that are optimal for differentiating cortical activation to subcortical regions would have resulted in missing virtually all significantly activated subcortical regions.

subjects' strategy was affected by doing a similar task before, we would expect that effect to be also present in the out-of-scanner BART performance among participants who completed "in-scanner first," i.e., smaller number of adjusted pumps during out-of-scanners task among participants who completed in-scanner BART first; (2) we would expect the hypothesized effect in (1) to have a greater magnitude in the out-of-scanner BART contrary to in-scanners BART, given that in-scanner BART, but not out-of-scanner BART had mock practice to wash-out any possible effects of the other task; and (3) this effect was very small and only trended toward significance.

No significant differences were observed for the in-scanner and out-of-scanner BART performance variables between participants who completed the behavioral and scan sessions "on the same day" versus "on separate days" for the in-scanner and out-of-scanner BART performance variables.

Correlations Between In-Scanner and Out-of-Scanner BART Performance

To test whether the same underlying processes were tapped in the original BART and the modified in-scanner version of the test, we examined cross-task correlations between performance variables (see Figure 1). We observed weak but significant positive correlations across the two tasks (ranging from.18 to.36, with $r = 0.35$ for the main risk-taking variable of *AdjustedPumps*), suggesting that these two paradigms are indicative of the same processes. We also computed correlations separately by sex and tested the significance of the difference between correlations for boys and girls. Correlation coefficients between in-scanner and out-of-scanner variables did not differ across boys and girls, except the correlation coefficient of *RT_PumpsExplosions* between in-scanner and out-of-scanner tasks trended toward significance and was greater in girls than in boys ($z = -1.60$, $P = 0.055$).

Sex Differences on Behavioral Performance for the In-Scanner and Out-of-Scanner BART

Behavioral performance of each sex (boys and girls) as well as a t-test of group differences is presented in Table 1. Group comparison revealed that for the out-of-scanner version of the BART, boys had a greater number of *AveragePumpsExplosions* ($t = 3.91$; $P < 0.001$) and a greater number of *AdjustedPumps* ($t = 3.21$; $P < 0.002$). On average, while boys had greater *N_Explosions* ($t = 3.42$; $P = 0.001$) compared to girls, girls had a greater *N_Cash-outs* ($t = -3.53$; $P = 0.001$) compared to boys. Regarding reaction times, girls pumped each balloon slower preceding cash-outs (*RT_PumpsCashouts*, $t = -5.01$, $P < 0.001$) and explosions (*RT_PumpsExplosions*, $t = -5.52$, $P < 0.001$) compared to boys.

For the in-scanner version of the BART, independent t-tests across groups showed that boys had a greater *N_Explosions* ($t = 4.31$; $P < 0.001$) and a greater number of *AdjustedPumps* ($t = 4.88$; $P < 0.001$) and *AveragePumpsExplosions* ($t = 2.42$;$P = 0.016$). Girls instead had a greater number of *N_Cashouts* ($t = -3.79$; $P < 0.001$). Girls pumped each balloon slower preceding cash-outs (*RT_PumpsCashouts*, $t = -2.28$, $P < 0.02$) and during cash-outs (*RT_Cashouts*, $t = -2.35$, $P < 0.02$) compared to boys. Note that given the in-scanner BART had a set duration (10 min) instead of a set number of balloons, the total number of balloons completed per subject varied. This total is presumed to be affected by the overall speed of the subjects and the number of pumps they were willing to make before cashing out. However, the number of completed balloons was not different across boys and girls.

fMRI Results

Categorical Design

Figure 2 displays the Cohen's d effect size estimates for the significant vertices in the categorical and parametric models. The cortical ROIs that were selected based on previous literature (BART studies in specific and risk-taking literature in general) in combination with the effect size cutoff are also highlighted in Figure 1 with outlines in green color. The selected cortical and subcortical ROIs are listed in Tables S8 and S9, respectively.

The cortical brain activations that were associated with risk taking (ChooseInflate) and taking the safe option (ChooseCashout) showed activations in some of the same parcels; however, these activations were greater while taking the safe option compared to risk taking: Risk taking (ChooseInflate) and choosing the safe option to cash-out (ChooseCashout) involved activations in superior parietal, inferior parietal, superior frontal, rostral middle frontal, and lateral occipital regions. The activations in the superior frontal, lateral orbitofrontal, and the insula were active during risky decision-making only; however, activations in these regions were not sensitive to the degree of the risk involved. Subcortical activations were observed in the right caudate in both conditions; the bilateral putamen, left caudate, and right thalamus were active only during risky decisions (ChooseInflate).

A broader set of regions were recruited during the receipt of negative outcome compared to the positive outcome of balloon inflation (155 anatomical regions identified for OutcomeExplode versus 7 for OutcomeInflate). Among the selected ROIs, activation in a parcel (r_FST) overlapping with the middle/inferior temporal/lateral occipital regions was present in both positive- and negative-outcome conditions, but greater during evaluation of negative outcomes. Activations in the lateral orbitofrontal gyrus, insula, caudal middle/superior/rostral middle frontal, inferior/superior parietal, caudal, and rostral ACC were exclusively recruited during the receipt of negative outcomes of balloon explosions (OutcomeExplode).

Parametric Design

The selected cortical and subcortical ROIs are listed in Table S10 (also see Figure 2). The parametrically modulated risk-taking condition (ChooseInflate) recruited the insula and lateral orbitofrontal cortex. The risk-taking condition with the parametric modulator recruited no additional regions that were not reported for the categorical model (Figure 2). Brain activation during the choice of cashing out (ChooseCashout) was modulated with the degree-of-loss avoidance (degree of risk). The regions that showed increased activation with increasing risk (ChooseInflate) including the posterior cingulate, superior parietal, inferior parietal, superior frontal, rostral middle frontal, insula, and caudal ACC.

Activations (Table S10, Figure 2) in the superior parietal, rostral middle frontal, inferior parietal, supramarginal, superior frontal, caudal ACC, posterior cingulate, precentral gyrus, lateral orbitofrontal cortex, insula, and rostral anterior cingulate increased with increasing degree of risk (that is increasing possibility of reward/loss) during the positive outcome (OutcomeInflate).

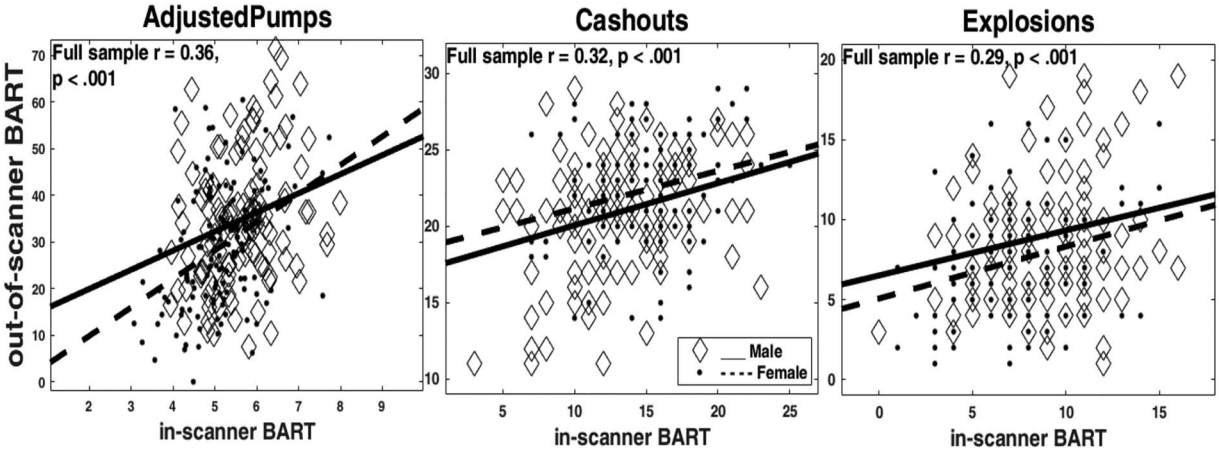

Outcome Variable	IS-OOS Correlations	Boys (df)	IS-OOS Correlations Boys	Girls (df)	IS-OOS Correlations Girls	Boys vs Girls (one-tailed)	
						Z-value	P-value
TotalPumps	0.361**	122	0.251**	131	0.380**	-1.13	0.129
N_Cashouts	0.320**	121	0.299**	125	0.273**	0.22	0.413
N_Explosions	0.286**	122	0.224*	130	0.275**	-0.43	0.334
AdjustedPumps	0.353**	122	0.253**	131	0.378**	-1.09	0.138
AveragePumpsExplosions	0.200**	122	0.201*	129	0.145	0.45	0.326
RT_Cashouts	0.186**	107	0.240*	116	0.147	0.71	0.239
RT_Pumps	0.194**	119	0.108	117	0.206*	-0.76	0.224
RT_PumpsCashouts	0.184**	117	0.166	114	0.153	0.10	0.460
RT_PumpsExplosions	0.184**	117	0.041	120	0.247**	-1.60	**0.055**

Notes: IS: in-scanner BART variables; OOS: Out-of-scanner BART variables, df: degrees of freedom, *p<0.05, **p<.01. Significance of the difference between correlation coefficients of boys and girl were calculated with the toolbox provided in: http://vassarstats.net/index.html

Figure 1. Scatterplots of the *AdjustedPumps*, *Cashouts*, and *Explosions* variables (upper panel). Pearson correlations between out-of-scanner (OOS) and in-scanner (IS) BART performance of boys and girls (lower panel).

A subset of regions (Table S10, Figure 2) that were identified in the negative-outcome condition (OutcomeExplode) also showed increasing activity as the degree of this loss increased. These regions included the caudal and rostral middle frontal, caudal and rostral ACC, insula and inferior, and superior parietal cortex. Activations in the superior frontal and precuneus were recruited distinctly in response to increasing levels of risk during negative outcomes.

Regions that were active only in the positive-outcome condition included right superior frontal, right superior parietal, right rostral middle frontal, right orbitofrontal, left rostral anterior cingulate, left supramarginal, and left insula. The aforementioned regions showed bilateral activations in the positive-outcome condition compared to unilateral activations in the negative-outcome condition. The right postcentral and right precuneus instead were only active in the negative-outcome condition.

Sex Differences in Selected ROIs

In the categorical design, the amplitude of the BOLD responses from 10 of the 33 selected ROIs in the OutcomeExplode contrast were greater for girls than boys (see Figure 3). These ROIs overlapped with the inferiorparietal, insula, lateral occipital/inferior temporal, inferiorparietal/supramarginal, lateralorbitofrontal, and rostralmiddlefrontal/parstriangularis regions. Within subcortical areas, girls compared to boys had greater activity only in the right caudate during ChooseCashout condition.

In the OutcomeExplode contrast of the parametric design, the amplitudes of the BOLD response from 5 of the 15 selected ROIs were greater for girls compared to boys. These ROIs overlapped with the caudal middle frontal/precentral, lateral occipital/inferior temporal, supramarginal, superiorparietal, and precuneus/isthmuscingulate regions. Additionally, in the OutcomeInflate contrast, the BOLD response of the caudal anterior cingulate/superior frontal region was greater for boys than girls. Girls instead had greater BOLD response in the middletemporal/lateraloccipital/inferior temporal, and posterior cingulate/isthmuscingulate regions in the ChooseCashout contrast. Previous reports showed sex differences in the amount of movement during fMRI (Yuan et al. 2009). Similarly, movement during the BART task was significantly different across boys and girls (boys> girls, $t = 3.297$, $P = 0.001$). Therefore, we tested if our findings of sex differences in the selected ROIs remained significant after correcting for differences in the amount of movement. Except for a few ROIs (2 out of 33 analyzed ROIs), sex differences remained significant across boys and girls (for details, see Supplementary Materials).

Table 1 Mean scores and SDs for the behavioral performances of boys and girls in the out-of-scanner (OOS) and in-scanner (IS) BART

Behavioral outcomes	Average (mean (SD))	Boys (mean (SD))	Girls (mean (SD))	Boys versus girls (*P*-value)	Boys versus girls (Cohen's d)
Out-of-Scanner BART					
TotalPumps	859.50 (316.83)	928.8 (312.26)	794.43 (308.29)	0.001	0.43
N_Cashouts	21.79 (3.68)	20.96 (3.84)	22.56 (3.37)	0.001	0.44
N_Explosions	8.25 (3.65)	9.04 (3.84)	7.50 (3.31)	0.001	0.43
AdjustedPumps	31.80 (13.67)	34.59 (13.78)	29.18 (13.08)	0.002	0.40
AveragePumpsExplosions	21.76 (7.89)	23.71 (8.56)	19.94 (6.74)	<0.001	0.49
RT_Cashouts	1056.35 (317)	1044.59 (314.85)	1067.56 (320.04)	0.573	0.07
RT_Pumps	356.29 (129)	314.50 (111.53)	398.77 (132.65)	<0.001	0.69
RT_PumpsCashouts	369.83 (134.94)	328.60 (117.20)	411.75 (139.29)	<0.001	0.65
RT_PumpsExplosions	317.16 (118)	277.44 (98.07)	356.24 (123.21)	<0.001	0.71
In-Scanner BART					
Balloons completed	22.23 (2.58)	22.64 (2.43)	22.91 (2.70)	0.202	0.11
N_Cashouts	14.03 (4.00)	13.08 (4.16)	14.94 (3.63)	<0.001	0.48
N_Explosions	8.15 (3.05)	8.97 (3.08)	7.39 (2.82)	<0.001	0.54
% Explosion rate	36.78 (14.58)	40.88 (14.78)	32.95 (13.34)	<0.001	0.56
AdjustedPumps	5.37 (.87)	5.63 (.84)	5.12 (.83)	<0.001	0.61
AveragePumpsExplosions	5.59 (.75)	5.70 (.70)	5.48 (.79)	0.016	0.29
RT_Explosions	742.78 (306.05)	755.32 (328.12)	730.93 (284.46)	0.534	0.08
RT_Cashouts	661.70 (235.82)	624.38 (208.46)	695.71 (254.34)	0.020	0.31
RT_Pumps	837.06 (280.18)	786.36 (247.31)	865.40 (292.98)	0.019	0.29
RT_PumpsCashouts	831.16 (286.17)	791.95 (252.74)	868.53 (277.94)	0.024	0.29
RT_PumpsExplosions	830.48 (303.64)	792.71 (290.54)	865.93 (312.40)	0.056	0.24

Notes. RT: reaction times, N: number of events, SD: standard deviations, Cohen's $d = (M2 - M1/SD_{pooled})$, $SD_{pooled} = \sqrt{((SD_1{}^2 + SD_2{}^2)/2)}$, based on https://www.socscistatistics.com/effectsize/default3.aspx

Sex Differences in all Parcels and Segments

Figure 4 displays the results of our exploratory analysis on sex differences across whole parcels and segments in the brain. The regions that showed significant sex differences are also listed in Tables S11 and S12 (see Supplementary Materials). Similar to the findings of sex differences in the selected ROIs, the amplitude of the BOLD response in the OutcomeExplode contrast in both designs was greater for girls than boys. The regions that showed sex differences in both designs included insula, lateral orbitofrontal, pars triangularis/opercularis (IFG), inferior parietal, parahippocampus, and precuneus (see Supplementary Materials for a complete list and corresponding HCP-MMP1.0 parcels). Within the subcortical regions, left putamen in the categorical design and left caudate, left pallidum and right caudate in the parametric design showed greater BOLD response in girls than in boys. No regions in either contrast or design showed greater activation in boys than in girls.

Discussion

In the present study, we examined neural correlates of two phases of decision-making under risk: risky (ChooseInflate) versus risk-averse (ChooseCashout) choices and evaluation of positive (OutcomeInflate) versus negative outcomes (OutcomeExplode) in a large sample of adolescents. Our primary goal was to characterize patterns of brain activation associated with these distinct processes. We were also interested in whether the same underlying cognitive processes were tapped in the scanner (Rao et al. 2008) version of the task in which the amount of monetary gain per pump increased with each subsequent pump and, hence, with increasing risks. In contrast, in the original version (Lejuez et al. 2002) of the task, the gain was fixed for all pumps regardless of the increasing risk. Specifically, we investigated whether parameters of performance in the two paradigms are correlated. Last, we studied whether behavioral and neural responses to risk differed across sex.

Risky and Risk-Aversive Decisions

One of the most significant findings to emerge from this study was the prominent activation of insula during risky decisions, but also its coactivation with increasing levels of risk during risk-averse decisions. The anterior insular cortex (AIC), a key hub in the salience network (SN), is known for its role in subjective feelings, emotional awareness (Craig 2009), and risk anticipation (Rudorf et al. 2012). Besides detecting and directing attention to salient stimuli, the SN network has been hypothesized to be involved in recruiting other networks, mainly activating the frontoparietal central executive network to facilitate access to attention and working memory resources when a salient event is detected (Menon and Uddin 2010). Therefore, the AIC has been viewed as an integrative hub, which processes arousal signals, then projects this information to task and context-relevant brain networks (Smith et al. 2014), but also processes a mismatch in risk prediction following a choice (Preuschoff et al. 2008; Rudorf et al. 2012). Our findings are consistent with the hypotheses that in adolescents in situations where the degree of risk gradually increases, the involvement of the AIC together with the cortical regions (including the OFC, ACC, ventromedial prefrontal cortex (vmPFC) and DLPFC) may play a central role in deciding to take more risks or to terminate the behavior, rather than the subcortical and cortical interactions, as we discuss below.

Sequential choice reactions invoke a sense of escalating tension (Schonberg et al. 2011) and require ongoing calculations of the trade-off between current cash-out value and the risk/reward associated with choosing the risky option. In our study,

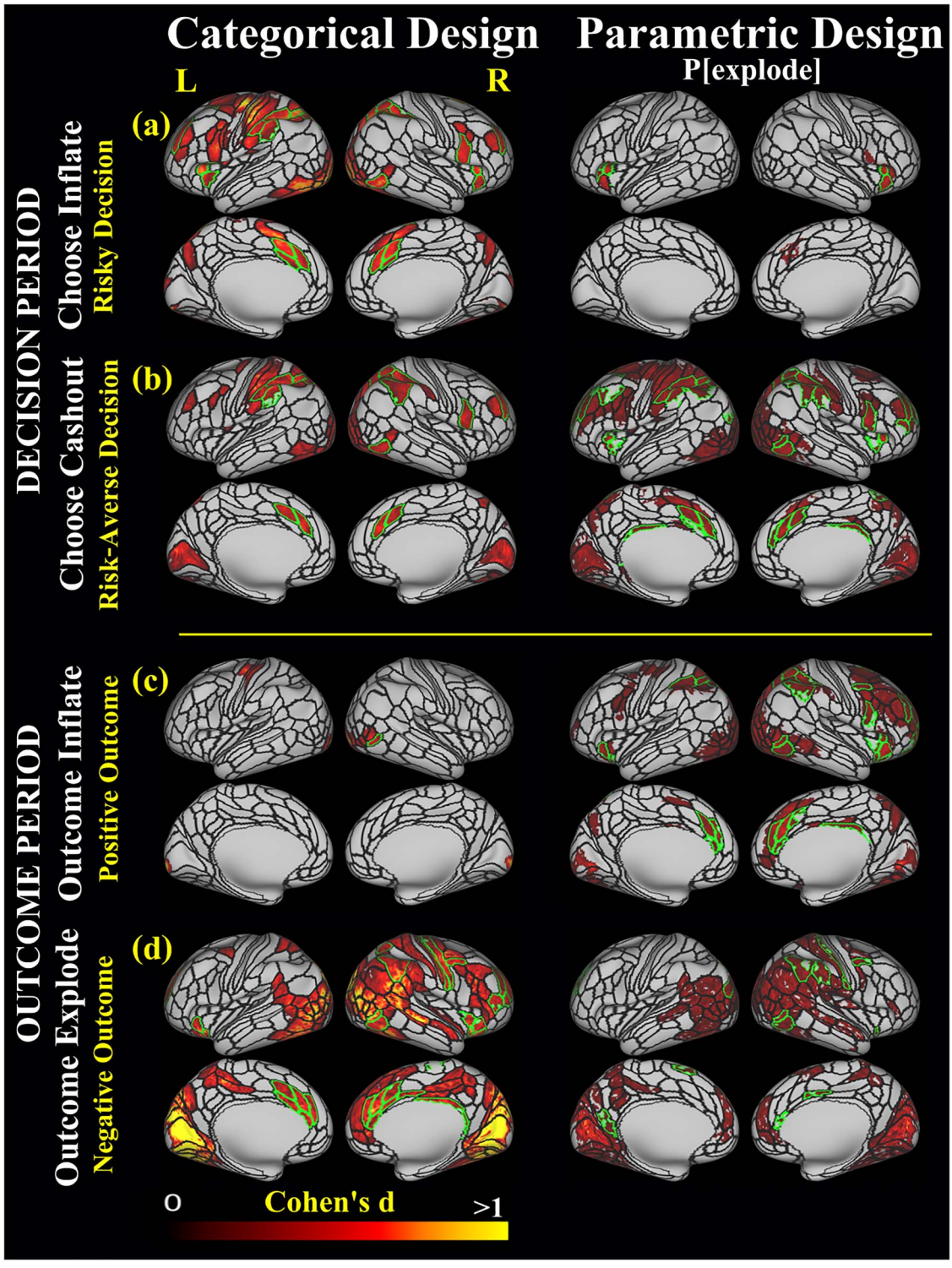

Figure 2. Cortical regions with significant brain activation (masked by FDR-corrected activation map, $P < 0.05$) that are also above our Cohen's d criteria (Cohen's $d > 0.35$ for categorical and Cohen's $d > 0.2$ for parametric design) in the categorical and parametric model related to the two phases of the BART, decision-making and outcome (feedback): (a) risky decision (ChooseInflate); (b) risk-averse decision (ChooseCashout), (c) positive outcome (OutcomeInflate; successful balloon inflation and monetary gain); (d) negative outcome (OutcomeExplode; balloon explosion and no money). **Black** outlines display the HCP-MMP1.0 parcellation. **Green** outlines demarcate the HCP-MMP1.0 parcels that contained an ROI that was selected for further analysis. Subcortical regions that were selected as ROIs in the categorical and parametric designs are listed in Supplementary Tables S9 and S10, respectively.

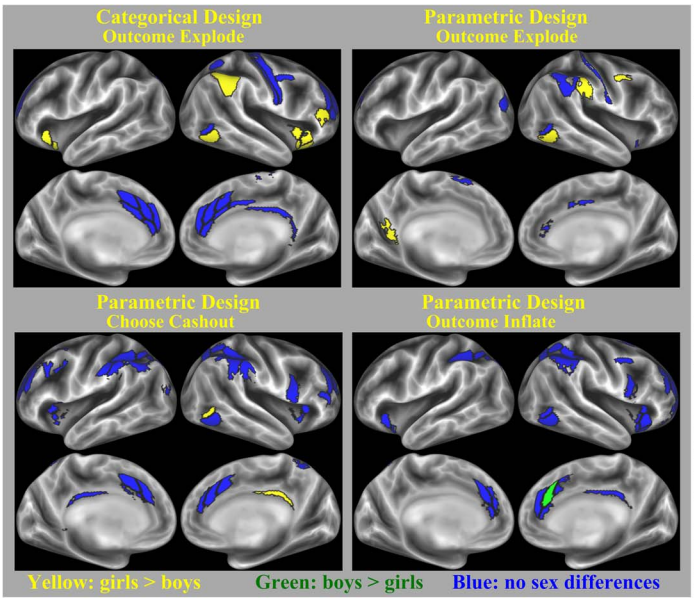

Girls > Boys		
Categorical Design – Outcome Explode		
R_ IP0	inferiorparietal	$t(252)$= -1.970, p= .050
R_AAIC	insula	$t(247)$= -2.340, p= .020
R_PH	lateraloccipital/inferior temporal	$t(244)$= -2.202, p= .029
R_PFm	inferiorparietal/supramarginal	$t(245)$= -2.332, p= .021
L_AAIC	insula	$t(244)$= -2.153, p= .032
R_AVI	lateralorbitofrontal/insula	$t(251)$= -3.098, p= .002
L_AVI	lateralorbitofrontal/insula	$t(246)$= -2.968, p= .003
R_MI	insula	$t(247)$= -2.792, p= .006
R_IFSa	rostralmiddlefrontal/parstriangularis	$t(247)$= -2.498, p= .013
R_47s	lateralorbitofrontal	$t(244)$= -1.988, p= .048
Categorical Design – Choose Cashout		
	R caudate	$t(237)$= -2.384, p= .018
Parametric Design – OutcomeExplode		
R_55b	caudalmiddle frontal/precentral	$t(243)$= -2.896, p= .004
R_PH	lateraloccipital/inferiortemporal	$t(230)$= -2.608, p= .010
R_PF	supramarginal	$t(234)$= -1.993, p= .047
L_IPS1	superiorparietal	$t(234)$= -2.272, p= .024
L_POS1	precuneus/isthmuscingulate	$t(233)$= -3.116, p= .002
Parametric Design – ChooseCashout		
R_FST	middle/inferior temporal/lateraloccipital	$t(237)$= -2.346, p= .020
R_RSC	posteriorcingulate/isthmuscingulate	$t(236)$= -2.533, p= .012
Boys > Girls		
Parametric Design – OutcomeInflate		
R_a32pr	caudal anteriorcingulate/superiorfrontal	$t(247)$ = 2.024, p = .044

L: left; R: right

Figure 3. Cortical regions with significant sex differences among the selected ROIs in the categorical and parametric models. Yellow parcels display the regions with greater activation in girls than boys; green parcels display the regions with greater activation in boys than girls. Blue parcels represent regions with no differences in activation between boys and girls. Only contrasts including regions that showed significant sex differences are displayed here.

the level of activation in the AIC increased with parametrically increasing level of risk during risky decisions, consistent with its purported role in the integration of arousal signals and in estimating risks with increasing stakes. More interestingly, greater degree of risk tracking in the insula was associated with greater number of risk-averse decisions (cashing-out) and less risk taking (a fewer number of pumps preceding cash-outs) (see Supplementary Table S14). It is important to note that although neural responses related to risky/risk-averse decisions were modeled for the period preceding the response, the decision may be made before this period, and the decision period may represent risk anticipation and execution of the risky/risk-averse choices. In contrast, choosing the safe option (risk-averse decisions) that avoided greater possible losses compared to smaller ones engaged greater activations in regions that are part of the two major executive networks, namely attention (dorsal attention) and cognitive control (frontoparietal) networks, including activations in anterior and medial intraparietal regions and caudal and rostral middle frontal areas (also known as the DLPFC). The hub model of the AIC proposes that after processing and interpreting physiological signals, AIC projects this information to the specific brain networks, each playing a part in achieving the desired behavioral response (Craig 2009). Therefore, our findings suggest the possibility that while the AIC keeps track of somatic sensations about the increasing risk, the two other executive networks may play a major role in transitioning from risky to safer choices.

While research in adolescent decision-making has largely focused on prefrontal and striatal regions, the possible role of the AIC and its maturation in adolescent risk taking has been proposed in a recent theoretical work (Smith et al. 2014). The author suggested that not only the adult-like AIC and striatal connections but also the still-developing connectivity from prefrontal regions to the AIC and striatum may result in difficulty in integrating affective and nonaffective information and contribute to the inability of adolescents to engage self-regulatory processes during risky decision-making. Our finding of AIC sensitivity to the escalating levels of risk is in line with a previous observation (Duijvenvoorde et al. 2015) that insula activity tracked increasing risks in adolescents (16–19 years old). Moreover, the same study found that risk-averse adolescents showed heightened activation in the right insula, IFG, and dmPFC. In an adult sample (age 18–23 years old), Fukunaga et al. (2012) showed decreasing activation in the AIC and increasing activity in vmPFC with increasing degree of risk during risk taking, while the same AIC region showed increased activity while making safe choices. Similarly, Paulus et al. (2003) reported that the degree of insula activation was related to the probability of selecting a "safe" response following a punished response (mean age 38 years old) (Paulus et al. 2003). While the AIC is involved in processing affective information and risk anticipation, the vmPFC has been found to be involved in the integration of information about value and outcome probability during decision processes under risk that might have a role in cost/benefit evaluations (Mcguire and Kable 2015). The functional role of the DLPFC in decision-making instead has been implicated as self-control and modulation of risk attitudes (Hare et al. 2009). The inconsistent findings between the adolescent (current one) and adult studies (Paulus et al. 2003; Fukunaga et al. 2012) may be due to a developmental change, reflecting a maturational transition from affective processing to a cost-benefit evaluation while making decisions involving risk. Due to the immaturities in the brain, greater involvement of the AIC might be required in adolescents for arousal signals to reach the required threshold to initiate harm avoidance processes, this could possibly explain why adolescents are more likely to take greater risks before switching to safer options. Although integration of these aversive signals and cost-benefit evaluations are important for the decision to change strategy (deciding to cash out after a number of inflations), previous experimental work suggests that it is the

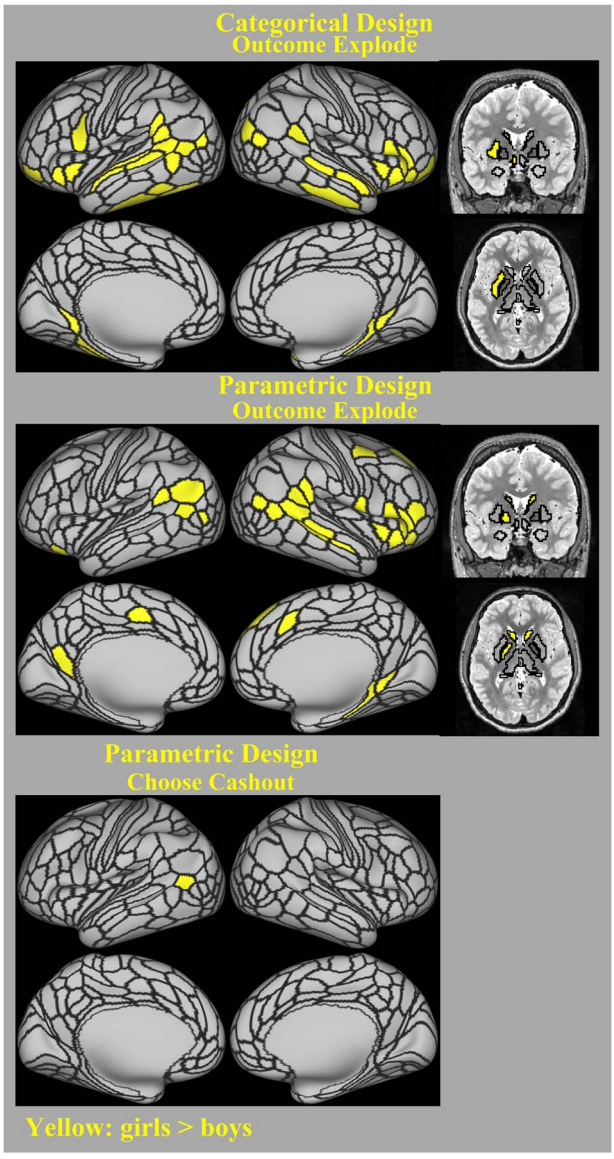

Figure 4. Regions with significant sex differences among all the cortical HCP-MMP1.0 parcels and subcortical Freesurfer segments in the categorical and parametric models (FDR-corrected, $P < 0.05$). Yellow parcels display the regions with greater activation in girls than boys (no parcels/segments showed greater activation in boys than girls). Only contrasts that showed significant sex differences are displayed here.

DLPFC that executes this switch (Knoch et al. 2006; Fecteau et al. 2007).

Contrary to previous reports of ventral striatum involvement during risky decisions (Bjork and Pardini 2015; Morales et al. 2018), we found the areas that are part of the dorsal striatum to be strongly activated during both risky (ChooseInflate, caudate) and risk-averse (ChooseCashout, caudate and putamen) decisions in adolescents. The involvement of ventral striatal activation during risk-averse decisions has only been reported in children but not in adults or adolescents (Paulsen et al. 2011). Moreover, the involvement of ventral striatal activation directly in risky decisions or indirectly through processing of increasing rewards might be weakened in the current sample given that a recent large-scale study identified the age of 16 as the time of peak ventral activation during reward processing (Schreuders et al. 2018), contrary to earlier reports of 14–15 years olds (Doremus-Fitzwater et al. 2010; Galvan 2010). Alternatively, due to the nature of the task, participants may need to evaluate implicit probability-related information to a greater extent than explicit reward information during decision-making in the current study. Previous research has shown that while the ventral striatum is linked to magnitude information, the dorsal striatum is correlated with probability information (Berns and Bell 2012). Given in the current task, subjects need to process probability based on implicit information, this task may require greater resources and greater involvement of dorsal activation. However, the dissociation of probability and magnitude signals is difficult to tease apart due to interdependency of risk probability and reward magnitude in the current task. It has been shown that individuals evaluate probability and magnitude information separately and then integrate the two pieces of information before making a choice (Berns and Bell 2012). ACC has been proposed as a target region where the multiplication of these two dimensions of information might be taking place (Berns et al. 2008). However, activation in the dorsal striatum did not increase at later stages of balloon inflation compared to earlier pumps, suggesting that the dorsal striatal regions do not process the magnitude of the risks/rewards while making risky decisions. Overall, our findings suggest that the choice of risky or safe options in adolescence may be guided by processing of somatic emotional arousal signals via insula, rather than increased sensitivity to the magnitude of risks/rewards.

The sensitivity of salience and dorsal attention networks to the changes in the levels of possible losses during the choice of safe options may imply that subjective evaluation of the reward/loss is important in the decision to change strategy during risk taking. This trade-off between value and risk inherent in sequential risk-taking paradigms mimics the findings in delay discounting paradigms, in which people switch between options when loss in value is too high. Current findings and previous research suggest that this evaluation might involve frontal and parietal regions as well as the insula and ACC. Interestingly, and in line with our findings, in a study by Helfinstein et al. (2014), brain networks of cognitive control (bilateral parietal and motor regions, the anterior cingulate cortex, bilateral insula, and bilateral lateral OFCs) were found to increase activity prior to avoiding a risk (selecting the safe option) (Helfinstein et al. 2014). Increased activity in these regions also successfully predicted initiation of a safe choice. The authors concluded that the engagement of cognitive control processes may be necessary to shift to a safer option.

Our findings regarding increased activation in these networks with increasing degree of possible loss suggest that risk aversion signals in the adolescent brain should be studied in relation to the magnitude of the loss avoided. In a cross-sectional study, Insel and Somerville (2018) identified a quadratic dip in anterior insula during loss-magnitude tracking in adolescents. Given that adolescents are more tolerant under aversive conditions, they can tolerate a greater degree of risk before switching to a safer option. In the literature, there have been controversial findings regarding if loss aversion does appear for smaller losses or not. To address this controversy, Mukherjee et al. (2017) studied loss aversion under high- and low-monetary values and found that loss aversion was observable only at higher magnitudes (Mukherjee et al. 2017);

this threshold might be even higher for adolescents. Another study showed that magnitudes of choices moderated people's decisions for low- versus high-stake gambles (Weber and Chapman 2005).

Evaluation of Positive and Negative Outcomes Following Risky Choices

A second comparison in our study was between the evaluation of positive and negative outcomes following the risky choices under two conditions: The first approach modeled the neural response as if each risky decision had the same levels of potential gain and loss (categorical model). The second approach investigated how neural response to positive and negative outcomes changed as a function of increasing risk faced by the decision maker at the choice period (parametric model). Our findings suggest that processing negative outcomes involves a greater network and is subject to sex effects. Several regions including the insula, lateral OFC, middle, rostral (overlapping with DLPFC), and superior frontal areas, and rostral and caudal ACC showed significant activation only in the negative-outcome condition. The decision maker takes a risk with the expectation that the possibility of a loss does not yet outweigh the possibility of a gain. Therefore, following a choice, the discrepancy between the subjective (or predicted) level of risk and the actual outcome needs to be used to update the decision maker's risk estimate, requiring the involvement of additional regions to achieve this task. While the likely role of the ACC during a negative-outcome evaluation is performance monitoring (Javadi et al. 2014), the increased activation in the DLPFC and the medial cortex are more likely to involve adjusting strategies to increase performance.

Brain responses engaged during the negative-outcome condition also showed sex differences, with girls showing greater activation than boys, largely in the insula and lateral orbitofrontal cortex. Sex differences observed in the insula might be driven by the tendency of girls toward greater risk-averse responses (fewer inflations and more cash-outs during the task). Rudorf et al. (2012) found elevated response to negative risk-prediction errors in the insula among risk averters compared to risk seekers. The authors suggested that elevated risk-prediction error signals in risk averters lead to overestimation of prospective risk. Risk-aversive preferences of girls observed in the current study together with greater involvement of the insula in girls may suggest a difference in risk-prediction-error processing but not in risk anticipation across girls and boys. Moreover, the OFC has been shown to have a role in interpreting feedback from a particular trial within the broader context of outcome history (Tsuchida et al. 2010). Therefore, the increased activation during the negative-outcome period in the aforementioned regions might be related to a heightened neural sensitivity toward adversity in girls.

Similar to our findings, in an fNIRS study, Cazzell and colleagues (2012) found greater activity in the DLPFC (rostral middle frontal) in adult females compared to males (25–44 yrs) in the negative-, but not in positive-outcome condition. It is important to note that the imaging modality used in the Cazzell et al. (2012) study cannot capture activity within medial wall or deeper cerebral structures, which explains why their study specifically focused on the lateral DLPFC structure. In the current study with a much larger sample size and a different imaging modality, we were able to identify greater activity in girls in a broader set of regions encompassing the inferior parietal, lateral orbitofrontal, and insula regions, though no sex effects on striatal activity were observed. These observed sex differences may be due to the developmental lag in cortical regions, as previous studies suggest faster functional maturation of prefrontal cortical regions in females (Anokhin et al. 2000). It is also possible that these differences might be inherent sex differences rather than the result of a lag in brain development, which should be addressed in future longitudinal studies.

Conclusions and Limitations

Here, we conducted a comprehensive study of adolescent decision-making under risk in a large, well-powered population-representative sample using two analytical approaches, categorical and parametric. Decision-making under risk requires the decision maker to make a cost/benefit analysis to estimate the value of alternative options. The use of the parametric model helped us to understand the role of specific brain networks that are involved in decision-making, in relation to the anticipated value of losses and gains. Our findings revealed that during risky decisions, the AIC tracked the degree of risk involved. Moreover, regions that are part of the dorsal attention and cognitive control networks were involved to a greater extent in risk-averse decisions. Therefore, our findings suggest that risky and risk-averse decisions in the adolescent brain should be studied in relation to the magnitude of risk involved/loss avoided. Interventions to reduce risk taking may target adolescents showing deficits in anticipatory emotional responses, which may be related to insensitivity to future consequences (Bechara et al. 1994). Moreover, our finding of sex differences in the cortical processing of negative outcomes may have different implications in boys and girls. While blunted response to negative outcomes may increase feelings of invulnerability in boys, greater sensitivity to negative outcomes in girls may put them at increased risk for anxiety and depression (Reyna and Farley 2006). Our findings can be utilized for the identification of risk for these conditions in adolescents in order to reduce unhealthy behaviors with potential negative long-term consequences.

However, we note a number of limitations: although our sample is large by the standards of neuroimaging studies, it was composed of MZ and DZ twins, allowing dependencies in the data. To overcome this limitation, we used statistics that reflect the paired structure of the data to create group activation maps. However, some of our exploratory correlation analyses might have been inflated due to our sample composition. Moreover, in this study, neural correlates of risky decisions were assessed in cash-out trials only (i.e., when balloon inflations were followed by cash-outs). This choice was driven by a concern that the inclusion of explosion trials may bias the estimate of risk-related neural activity. While cash-out trials represent the full extent of the risk participants are willing to take (i.e., until the point they make a decision to cash out), in the explosion trials, the number of pumps is artificially truncated. Since in the current task, both objective and subjective risks of balloon explosion increased with subsequent pumps, such a truncation could result in a systematic exclusion of the most risky decisions from the analysis (i.e., balloon inflation preceding a cash-out) and, consequently, underestimation of risk-related neural activity. However, we acknowledge that cash-out trials may also be subject to a bias because if a cash-out trial is preceded by an explosion trial, carry-over effects from a previous trial may occur— that is, subjects may be more cautious following explosion trials. Many previous MRI studies of BART have included pumps

preceding both cash-outs and explosions[2]. This difference in the analytical approach should be taken into consideration while comparing the results of the current study and previous studies. The influence of previous outcomes (Kohno et al. 2015) or even intrinsic fluctuations of brain activity (Chew et al. 2019) on decision-making under risk is a complex issue that should be further clarified in studies designed to probe the within-subject dynamics of decision-making and its underlying brain activity (e.g., using computational modeling). Furthermore, the subcortical segmentation utilized in this study (Desikan-Killiany atlas, Desikan et al. 2006) divides the cerebellar volume into the left and right hemispheres. Therefore, although cerebellar regions showed significant activations with Cohen's d value $> .2$, neither of these parcels survived our ROI selection criteria that activation was present in 50% of the segment. For interested readers, a voxel-wise representation of these activations are provided in Supplementary Figure S6. Future research should look at subcortical and cerebellar activation in a more refined manner. Lastly, we acknowledge that our conclusions are based on a specific risk-taking task and may not generalize to a broader range of paradigms.

Future Directions

Future research that aims to dissociate the specific functional role of these regions in decision-making can benefit from the use of computational models, in which individual decision-making styles and strategies can be studied in relation to brain activations (Wallsten et al. 2005). Moreover, future studies should aim to test the influence of sex hormones or pubertal status on the observed differences in neural correlates of negative-outcome evaluation across boys and girls. Our study also showed that the individual differences in the scanner version of the task weakly but significantly correlated with the behavioral version, suggesting a similar construct was used in both modalities. Although the behavioral version of the BART has been found to be highly reliable ($r = 0.77$, White et al. 2008), long-term longitudinal stability in early adolescence was only fair ($r = 0.48$, but highly significant), which can be attributed to significant developmental changes in behavior during that period (Anokhin et al. 2009). Furthermore, studies investigating the reliability of brain responses measured by this task are largely lacking. Future studies should also aim to test the reliability of brain responses involved in risky decision-making.

Supplementary Material

Supplementary material is available at *Cerebral Cortex* online.

Funding

Research reported in this publication was supported by Eunice Kennedy Shriver National Institute of Child Health and Human Development (NICHD) of the National Institutes of Health under award number R01HD083614.

2 Among fMRI BART literature, neural correlates of risky decisions were assessed in cash-out trials only in six studies (Qu et al. 2015; Schonberg et al. 2012; Telzer et al. 2013a, 2013b, 2014, 2015), while five other studies presumably used all pumps (Claus and Hutchison, 2012; Fukunaga et al. 2012; Hulvershorn et al. 2015; Kohno et al. 2015; Rao et al. 2008), given that the authors refer to pumps instead of adjusted pumps in the description of their analysis of risky decisions.

Notes

The content is solely the responsibility of the authors and does not necessarily represent the official views of the National Institutes of Health. *Conflict of Interest:* None declared.

References

Anokhin AP, Golosheykin S, Grant J, Heath AC. 2009. Heritability of risk-taking in adolescence: a longitudinal twin study. *Twin Research and Human Genetics*. 12:366–371.

Anokhin AP, Lutzenberger W, Nikolaev A, Birbaumer N. 2000. Complexity of electrocortical dynamics in children: developmental aspects. *Developmental Psychobiology*. 36:9–22.

Benjamini Y, Hochberg Y. 1995. Controlling the false discovery rate: a practical and powerful approach to multiple testing. *Journal of the Royal Statistical Society, Series B*. 57:289–300.

Bechara A, Damasio A, Damasio H, Anderson S. 1994. Insensitivity to future consequences following damage to prefrontal cortex. *Cognition*. 50:7–15.

Benjamini Y, Yekutieli D. 2001. The control of the false discovery rate in multiple testing under dependency. *The Annals of Statistics*. 29:1165–1188.

Berns GS, Capra CM, Chappelow J, Moore S, Noussair C. 2008. Nonlinear neurobiological probability weighting functions for aversive outcomes. *NeuroImage*. 39(4):2047–2057.

Bjork JM, Pardini DA. 2015. Who are those "risk-taking adolescents"? Individual differences in developmental neuroimaging research. *Developmental Cognitive Neuroscience*. 11:56–64.

Bjork JM, Smith AR, Chen G, Hommer DW. 2010. Adolescents, adults and rewards: comparing motivational neurocircuitry recruitment using fMRI. *PLoS ONE*. 5:e11440.

Berns GS, Bell E. 2012. Striatal topography of probability and magnitude information for decisions under uncertainty. *NeuroImage*. 59:3166–3172.

Blankenstein NE, Crone EA, van den Bos W, van Duijvenvoorde AC. 2016. Dealing with uncertainty: testing risk- and ambiguity-attitude across adolescence. *Developmental Neuropsychology*. 41(1–2):77–92.

Blankenstein NE, Schreuders E, Peper JS, Crone EA, van Duijvenvoorde AC. 2018. Individual differences in risk-taking tendencies modulate the neural processing of risky and ambiguous decision-making in adolescence. *NeuroImage*. 172:663–673.

Boyer TW. 2006. The development of risk-taking: a multi-perspective review. *Developmental Review*. 26:291–345.

Casey BJ, Cannonier T, Conley MI, Cohen AO, Barch DM, Heitzeg MM, Soules ME, Teslovich T, Dellarco DV, Garavan H *et al*. 2018. The adolescent brain cognitive development (ABCD) study: imaging acquisition across 21 sites. *Developmental Cognitive Neuroscience*. 32:43–54.

Casey BJ, Jones RM, Hare TA. 2008. The adolescent brain. *Annals of the New York Academy of Sciences*. 1124:111–126.

Cauffman E, Shulman EP, Steinberg L, Claus E, Banich MT, Graham S, Woolard J. 2010. Age differences in affective decision making as indexed by performance on the Iowa gambling task. *Developmental Psychology*. 46:193–207.

Cazzell M, Li L, Lin ZJ, Patel SJ, Liu H.. 2012. Comparison of neural correlates of risk decision making between genders: an exploratory fNIRS study of the Balloon Analogue Risk Task (BART). *Neuroimage*. 62:1896–1911.

Chew B, Hauser TU, Papoutsi M, Magerkurth J, Dolan RJ, Rutledge RB. 2019. Endogenous fluctuations in the dopaminergic midbrain drive behavioral choice variability. *PNAS*. 116:18732–18737.

Claus ED, Hutchison KE. 2012. Neural mechanisms of risk taking and relationships with hazardous drinking. *Alcoholism, Clinical and Experimental Research*. 36:408–416.

Coalson TS, Essen DCV, Glasser MF. 2018. The impact of traditional neuroimaging methods on the spatial localization of cortical areas. *Proceedings of the National Academy of Sciences of the United States of America*. 115:E6356–E6365.

Craig ADB. 2009. How do you feel — now? The anterior insula and human awareness. *Nature Reviews. Neuroscience*. 10:59–70.

Desikan RS, Se F, Fischl B, Quinn BT, Dickerson BC, Blacker D, Buckner RL, Dale AM, Maguire RP, Hyman BT *et al*. 2006. An automated labeling system for subdividing the human cerebral cortex on MRI scans into gyral based regions of interest. *NeuroImage*. 31:968–980.

Doremus-Fitzwater TL, Varlinskaya EI, Spear LP. 2010. Motivational systems in adolescence: possible implications for age differences in substance abuse and other risk-taking behaviors. *Brain and Cognition*. 72:114–123.

Duijvenvoorde ACKV, Huizenga HM, Somerville LH, Delgado MR, Powers A, Weeda WD, Casey BJ, Weber EU, Figner B. 2015. Neural correlates of expected risks and returns in risky choice across development. *The Journal of Neuroscience*. 35:1549–1560.

Eaton D, Kann L, Kinchen S, Shanklin S, Flint K, Hawkins J, Harris W, Lowry R, McManus T, Chyen D *et al*. 2012. Youth risk behavior surveillance — United States, 2011. *Morbidity Mortal Weakly Report*. 61:1–162.

Ernst M, Paulus MP. 2005. Neurobiology of decision making: a selective review from a neurocognitive and clinical perspective. *Biological Psychiatry*. 58:597–604.

Eshel N, Nelson EE, Blair RJ, Pine DS, Ernst M. 2007. Neural substrates of choice selection in adults and adolescents: development of the ventrolateral prefrontal and anterior cingulate cortices. *Neuropsychologia*. 45:1270–1279.

Fecteau S, Pascual-leone A, Zald DH, Liguori P, Theoret H, Boggio PS, Fregni F. 2007. Activation of prefrontal cortex by transcranial direct current stimulation reduces appetite for risk during ambiguous decision making. *The Journal of Neuroscience*. 27:6212–6218.

Fukunaga R, Brown JW, Bogg T. 2012. Decision making in the balloon analogue risk task (BART): anterior cingulate cortex signals loss-aversion but not the infrequency of risky choices. *Cognitive, Affective, & Behavioral Neuroscience*. 12:479–490.

Galvan A. 2010. Adolescent development of the reward system. *Frontiers in Human Neuroscience*. 4:1–9.

Geier CF, Terwilliger R, Teslovich T, Velanova K, Luna B. 2010. Immaturities in reward processing and its influence on inhibitory control in adolescence. *Cerebral Cortex*. 20:1613–1629.

Glasser MF, Coalson TS, Robinson EC, Hacker CD, Harwell J, Yacoub E, Ugurbil K, Andersson J, Beckmann CF *et al*. 2016. A multi-modal parcellation of human cerebral cortex. *Nature*. 536:171–178.

Glasser MF, Sotiropoulos SN, Wilson JA, Coalson TS, Fischl B, Andersson JL, Xu J, Jbabdi S, Webster M, Polimeni JR *et al*. 2013. The minimal preprocessing pipelines for the human Connectome project. *NeuroImage*. 80:105–124.

Glimcher PW. 2008. Understanding risk: a guide for the perplexed. *Cognitive, Affective, and Behavioural Neuroscience*. 8(4):348–354.

Hare TA, Camerer CF, Rangel A. 2009. Self-control in decision-making involves modulation of the vmPFC valuation system. *Science*. 324:646–648.

Helfinstein SM, Schonberg T, Congdon E, Karlsgodt KH, Mumford JA. 2014. Predicting risky choices from brain activity patterns. *Proceedings of the National Academy of Sciences of the United States of America*. 111:2470–2475.

Huettel SA, Stowe CJ, Gordon EM, Warner BT, Platt ML. 2006. Neural signatures of economic preferences for risk and ambiguity. *Neuron*. 49:765–775.

Hulvershorn LA, Hummer TA, Fukunaga R, Leibenluft E, Finn P, Cyders MA, Anand A, Overhage L, Dir A, Brown J. 2015. Neural activation during risky decision-making in youth at high risk for substance use disorders. *Psychiatry Research: Neuroimaging*. 233:102–111.

Hunt M, Hopko DR, Bare R, Lejuez C, Robinson E. 2005. Construct validity of the balloon Analog risk task (BART) associations with psychopathy and impulsivity. *Assessment*. 12:416–428.

Insel C, Somerville LH. 2018. Asymmetric neural tracking of gain and loss magnitude during adolescence. *Social Cognitive and Affective Neuroscience*. 13(8):785–796.

Javadi AH, Schmidt DHK, Smolka MN. 2014. Differential representation of feedback and decision in adolescents and adults. *Neuropsychologia*. 56:280–288.

Jenkinson M, Beckmann CF, Behrens TEJ, Woolrich MW, Smith SM. 2012. FSL. *NeuroImage*. 62:782–790.

Jentsch JD, Taylor JR. 1999. Impulsivity resulting from frontostriatal dysfunction in drug abuse: implications for the control of behavior by reward-related stimuli. *Psychopharmacology*. 146:373–390.

Kim-Spoon J, Deater-Deckard K, Lauharatanahirun N, Farley J, Chiu PH, Bickel WK, King-Casas B. 2017. Neural interaction between risk sensitivity and cognitive control predicting health risk behaviors among late adolescents. *Journal of Research on Adolescence*. 27:674–682.

Knoch D, Gianotti LRR, Pascual-leone A, Treyer V, Regard M, Hohmann M, Brugger P. 2006. Disruption of right prefrontal cortex by low-frequency repetitive transcranial magnetic stimulation induces risk-taking behavior. *The Journal of Neuroscience*. 26:6469–6472.

Kohno M, Ghahremani DG, Morales AM, Robertson CL, Ishibashi K, Morgan AT, Mandelkern MA, London ED. 2015. Risk-taking behavior: dopamine D2/D3 receptors, feedback, and frontolimbic activity. *Cerebral Cortex*. 25:236–245.

Krain AL, Wilson AM, Arbuckle R, Castellanos FX, Milham MP. 2006. Distinct neural mechanisms of risk and ambiguity: a meta-analysis of decision-making. *NeuroImage*. 32:477–484.

Lee TMC, Chan CCH, Leung AWS, Fox PT, Gao J. 2009. Sex-related differences in neural activity during risk taking: an fMRI study. *Cerebral Cortex*. 19:1303–1312.

Lejuez CW, Aklin W, Daughters S, Zvolensky M, Kahler C, Gwadz M. 2007. Reliability and validity of youth version of the Ballon analogues risk task (BART-Y) in the assessment of risk-taking behavior among inner-city adolescents. *Journal of Clinical and Adolescent Psychology*. 36(1):106–111.

Levy I, Snell J, Nelson AJ, Rustichini A, Glimcher PW. 2010. Neural representation of subjective value under risk and ambiguity. *Journal of Neurophysiology*. 103:1036–1047.

Lejuez CW, Read JP, Kahler CW, Richards JB, Ramsey SE, Stuart GL, Strong DR, Brown RA, York N, Ramsey SE *et al*. 2002. Evaluation of a behavioral measure of risk taking: the balloon analogue risk task (BART). *Journal of Experimental Psychology. Applied*. 8:75–84.

Mcguire JT, Kable JW. 2015. Medial prefrontal cortical activity reflects dynamic re-evaluation during voluntary persistence. *Nature Neuroscience*. 18:760–766.

Menon V, Uddin LQ. 2010. Saliency, switching, attention and control: a network model of insula function. *Brain Structure & Function*. 214:655–667.

Morales AM, Jones SA, Ehlers A, Lavine JB, Nagel BJ. 2018. Ventral striatal response during decision making involving risk and reward is associated with future binge drinking in adolescents. *Neuropsychopharmacology*. 1884–1890.

Mukherjee S, Sahay A, Pammmi VSC, Srinivasan N. 2017. Is loss-aversion magnitude-dependent? Measuring prospective affective judgments regarding gains and losses. *Judgment and Decision making*. 12:81–89.

O'Donnell L, Agronick G, Duran R, Myint-U A, Stueve A. 2009. Intimate partner violence among economically disadvantages young adult woman: associations with adolescnet risk-taking and pregnancy experiences. *Perspectives on Sexual and Reproductive Health*. 41(2):85–91.

Paulsen DJ, Carter RM, Platt ML, Huettel SA, Brannon EM. 2011. Neurocognitive development of risk aversion from early childhood to adulthood. *Frontiers in Human Neuroscience*. 5:178.

Paulus MP, Rogalsky C, Simmons A, Feinstein JS, Stein MB. 2003. Increased activation in the right insula during risk-taking decision making is related to harm avoidance and neuroticism. *NeuroImage*. 19:1439–1448.

Preuschoff K, Quartz SR, Bossaerts P. 2008. Human insula activation reflects risk prediction errors as well as risk. *The Journal of Neuroscience*. 28(11):2745–2752.

Rao H, Korczykowski M, Pluta J, Hoang A, Detre J. 2008. Neural correlates of voluntary and involuntary risk taking in the human brain: an fMRI study of the balloon Analog risk task (BART). *NeuroImage*. 42:902–910.

Reyna VF, Farley F. 2006. Risk and rationality in adolescent decision making: implications of theory, practice and public policy. *Psychological Science*. 7(1):1–44.

Robinson EC, Garcia K, Glasser MF, Chen Z, Coalson TS, Makropoulos A, Bozek J, Wright R, Schuh A, Webster M. *et al*. 2018. Multimodal surface matching with higher-order smoothness constraints. *Neuroimage*. 167:453–465.

Rudorf S, Preuschoff K, Weber B. 2012. Neural correlates of anticipation risk reflect risk preferences. *The Journal of Neuroscience*. 32(47):16683–16692.

Schonberg T, Fox CR, Mumford JA, Congdon E, Trepel C, Poldrack RA. 2012. Decreasing ventromedial prefrontal cortex activity during sequential risk-taking: an FMRI investigation of the balloon analog risk task. *Frontiers in Neuroscience*. 6: 1–11.

Schonberg T, Fox CR, Poldrack RA. 2011. Mind the gap: bridging economic and naturalistic risk-taking with cognitive neuroscience. *Trends in Cognitive Sciences*. 15:11–19.

Schreuders E, Braams BR, Blankenstein NE, Peper JS, Güroğlu B, Crone EA. 2018. Contributions of reward sensitivity to ventral striatum activity across adolescence and early adulthood. *Child Development*. 89(3):797–810.

Silverman MH, Jedd K, Luciana M. 2015. Neural networks involved in adolescent reward processing: an activation likelihood estimation meta-analysis of functional neuroimaging studies. *NeuroImage*. 122:427–439.

Smith AR, Steinberg L, Chein J. 2014. The role of the anterior insula in adolescent decision making. *Developmental Neuroscience*. 36:196–209.

Steinberg L. 2004. Risk taking in adolescence: what changes, and why? *Annals of the New York Academy of Sciences*. 1021: 51–58.

Somerville LH, Jones RM, Casey BJ. 2010. A time of change: behavioral and neural correlates of adolescent sensitivity to appetitive and aversive environmental cues. *Brain and Cognition*. 72:124–133.

Telzer EH, Fuligni AJ, Lieberman MD, Galvan A. 2013a. The effects of poor sleep on brain function and risk taking in adolescence. *NeuroImage*. 71. doi: 10.1016/j.neuroimage.2013.01.025.

Telzer EH, Fuligni AJ, Lieberman MD, Galvan A. 2013b. Meaningful family relationships: neurocognitive buffers of adolescent risk taking. *Journal of Cognitive Neuroscience*. 25: 374–387.

Telzer EH, Fuligni AJ, Lieberman MD, Miernicki ME, Galvan A. 2015. The quality of adolescents peer relationships modulates neural sensitivity to risk taking. *Social Cognitive and Affective Neuroscience*. 10:389–398.

Telzer EH, Fuligni AJ, Lieberman MD, Galvan A. 2014. Neural sensitivity to eudaimonic and hedonic rewards differentially predict adolescent depressive symptoms over time. *PNAS*. 111:6600–6605.

Tisdall MD, Hess AT, Reuter M, Meintjes EM, Fischl B, van der Kouwe AJW. 2012. Volumetric navigators for prospective motion correction and selective reacquisition in neuroanatomical MRI. *Magnetic Resonance in Medicine*. 68: 389–399.

Tsuchida A, Doll BB, Fellows LK. 2010. Beyond reversal: a critical role for human orbitofrontal cortex in flexible learning from probabilistic feedback. *The Journal of Neuroscience*. 30:16868–16875.

Tymula A, Rosenberg Belmaker LA, Roy AK, Ruderman L, Manson K, Glimcher PW, Levy I. 2012. Adolescents' risk-taking behavior is driven by tolerance to ambiguity. *Proceedings of the National Academy of Sciences of the United States of America*. 109:17135–17140.

Qu Y, Galvan A, Fuligni AJ, Lieberman MD, Telzer EH. 2015. Longitudinal changes in prefrontal cortex activation underlie declines in adolescent risk taking. *Journal of Neuroscience*. 35:11308–11314.

Van Den Bos W, Hertwig R. 2017. Adolescents display distinctive tolerance to ambiguity and to uncertainty during risky decision making. *Scientific Reports*. 7:40962.

Van Leijenhorst L, Gunther Moor B, Op de Macks ZA, Rombouts SARB, Westenberg PM, Crone EA. 2010. Adolescent risky decision-making: neurocognitive development of reward and control regions. *NeuroImage*. 51:345–355.

Vigil P, Del Rio P, Carrera B, Aranguiz FC, Rioseco H, Cortes ME. 2016. Influence of sex steroid hormones on the adolescent brain and behavior: an update. *The Linacre Quarterly*. 83:308–329.

Wallsten TS, Pleskac TJ, Lejuez CW. 2005. Modeling behavior in a clinically diagnostic sequential risk-taking task. *Psychological Review*. 112:862–880.

Weber BJ, Chapman GB. 2005. Playing for peanuts: why is risk seeking more common for low-stakes gambles? *Organizational Behavior and Human Decision Processes*. 97:31–46.

White TL, Lejuez CW, Wit, De H. 2008. Test-retest characteristics of the balloon analogue risk task (BART). *Experimental and Clinical Psychopharmacology*. 16:565–570.

Winkler AM, Ridgway GR, Webster MA, Smith SM, Nichols TE. 2014. NeuroImage permutation inference for the general linear model. *NeuroImage*. 92:381–397.

Winkler AM, Webster MA, Vidaurre D, Nichols TE, Smith SM. 2015. Multi-level block permutation. *NeuroImage*. 123:253–268.

Yuan W, Altaye M, Ret J, Schmithorst V, Byars AW, Plante E, Holland SK. 2009. Quantification of head motion in children during various fMRI language tasks. *Human Brain Mapping*. 30(5):1481–1489.